Disneyland ride final design report

Structural Dynamics Research Corporation (SDRC)

Daniel Belongia
Adam Mayer
Donny Kuettel
Nasser M. Abbasi

EMA 542 Advanced dynamics
University Of Wisconsin, Madison
Fall 2013

Abstract

Dynamic analysis was completed for a new spinning ride as requested by Walt Disney Corporation. Detailed derivation of model was completed for the main structural elements using rigid body dynamics.

Critical section was identified and maximum stress calculated to insure that the member does not fail during operations and passengers acceleration does not exceed 6g.

Large software simulation program was completed to verify the model used and to allow selection of optimal design parameters.

Prepared by:

Dynamic design team
Structural Dynamics Research Corporation (SDRC)

Contents

List of Figures

List of Tables

1   Introduction

A four-member team at Structural Dynamics Research Corporation (SDRC) has completed the final design for a new spinning ride for Disneyland.

The ride features two non-collinear components of angular velocity. The head of each passenger will experience a maximum of $6g$ acceleration. Just before this acceleration is reached, the ride will enter steady state. During steady state, passengers will experience a small periodic fluctuation of acceleration that ranges between $4.8g$ and $6g$ but will not exceed $6g$. The ride can then enter the ramp down phase and starts to decelerate until it stops with smooth landing. All three phases of the ride have been simulated to insure the passengers will not exceed $6g$ during any of the phases. The ride is specifically designed to be light, safe, affordable, and fun. The following is an artist rendering showing loading the passengers in the cabinet before starting the ride Once the cabinet has reached the top of the support column, the ride will
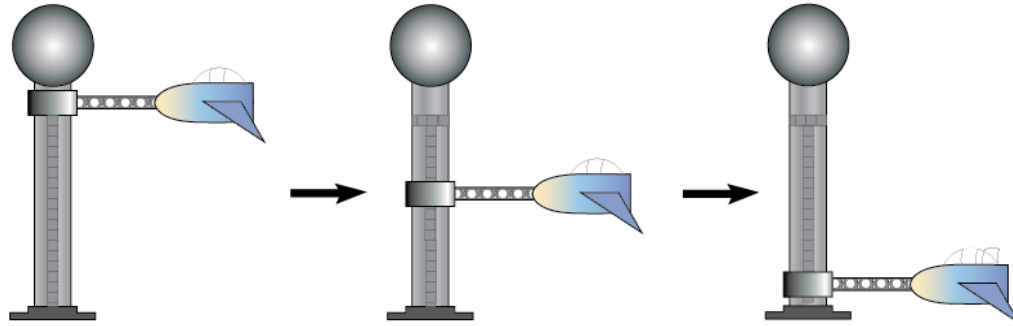
Figure 1: Artist rendering of ride after construction

start. Extensive simulation of the mathematical model of the dynamics of the model was performed to achieve an optimal set of design parameters in order to meet the design goals as specified in the customer requirements of a minimum weight and cost and at the same time insuring the structural members do not fail and that the passengers will safely achieve the $6g$ acceleration in reasonable amount of time. The conclusion section outlines the final design parameters found. The following diagram illustrates typical one revolution ride for illustrations that was generated by the simulator developed specifically for this design contract

Time history snap shot of typical ride revolution
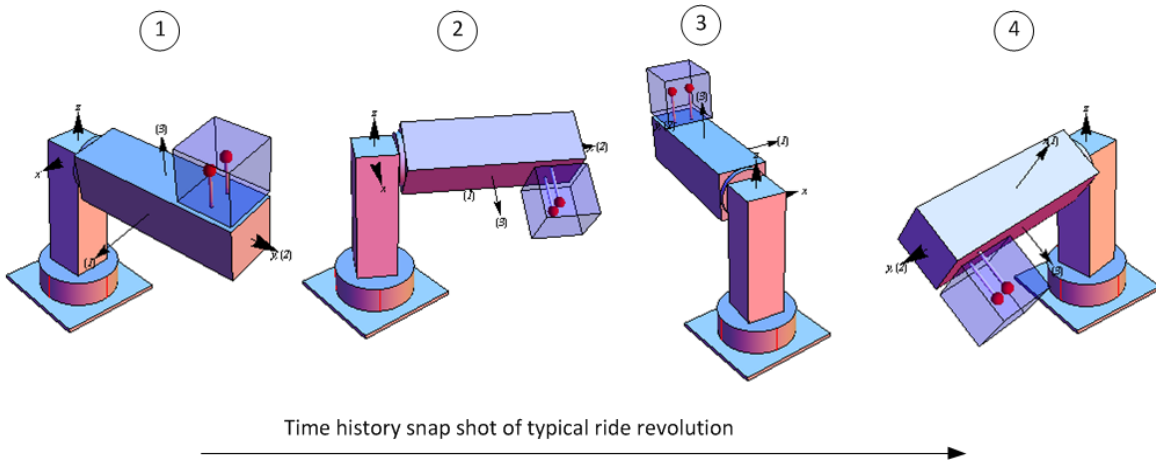
Figure 2: Illustrating typical dynamic movement over four time instances for one revolution

1.1 Gantt chart and history of design project

The design team followed the following timeline in the development of the report and the design. This is illustrated below using Gantt chart
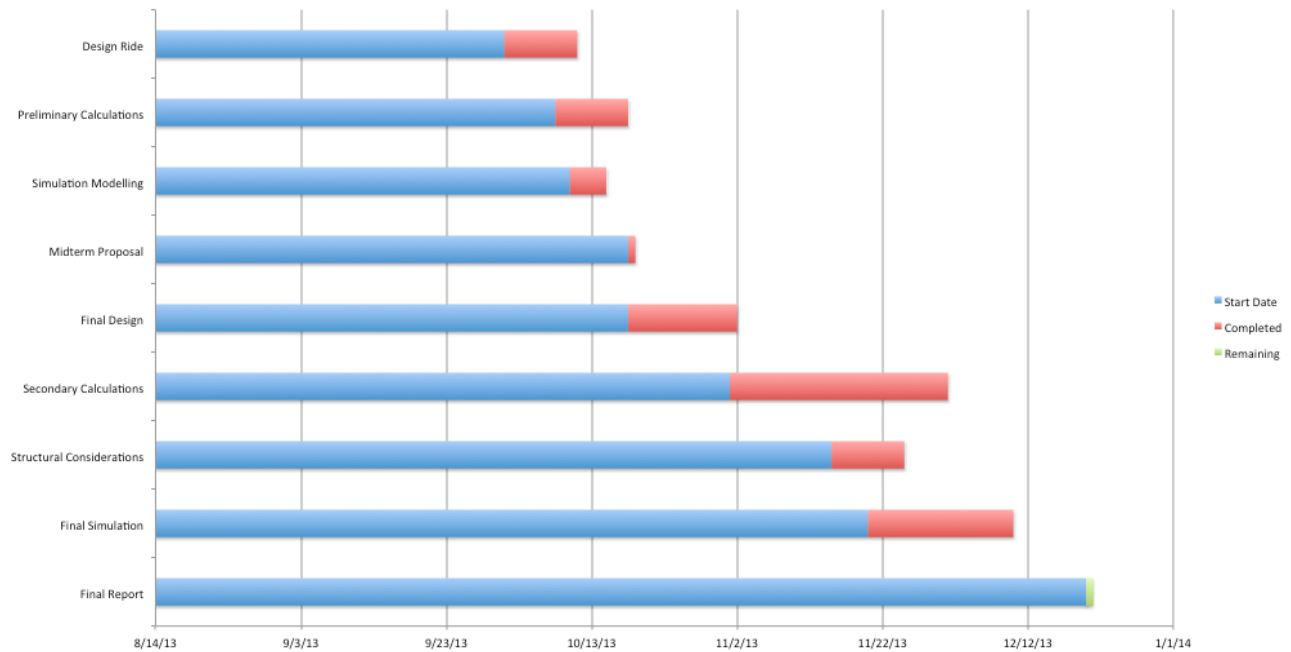
Figure 3: Time line used by the design team in the development of the final project report

2 Safety considerations

The flight simulator will be equipped with multiple safety measures to ensure that passengers will have a fun and exciting ride. In order to ride the flight simulator, each passenger must be at least 5 feet tall. This insures that the riders can be securely fastened into the seat. Assuming an average rider weight of 175 pounds, one single rider cannot weigh more than 350 pounds.

Any more weight will induce a moment on the main arm that might be considered unsafe. A factor of safety was factored into the building of the arm in case two riders combined weight to be more than 350 pounds. This additional weight accounts for the seating weight and the frame of the cabinet as well.

While the ride is in motion, each passenger will be harnessed into his or her seat via a 3-point harness. The harness will let the passengers fly upside-down while still secured in the cockpit. Since the flight simulator will be subject to $6g$ acceleration, complementary sick bags will be provided upon starting.

In case of a medical emergency of a passenger or if it has been determined that it is unsafe to ride mid-flight, an emergency stop will be activated which will bring the ride to an end. When activated, the ride will right itself upwards while bringing itself to a stop about the center of the ride. This is so when the ride stops, the passengers are not hanging upside down which would be unsafe.

2.1 Locations of possible failure in the structure

Four critical sections in the structure were identified as possible failure sections. These are shown in the following diagram. They ranked from 1 to 4 in order of possible first to fail. Hence section 1 is the one expected to fail first.

From bending moment diagram generated during initial runs of simulation it was clear that the bending moment at section 1 was much larger than section 3. This agrees with typical cantilever beam model which the above have very close similarity when considering the cabinet as additional distributed load on the beam. However, this is a dynamic design and not static, hence time dependent bending moment and shear force diagrams are used to validate this. These diagrams were not included in the final
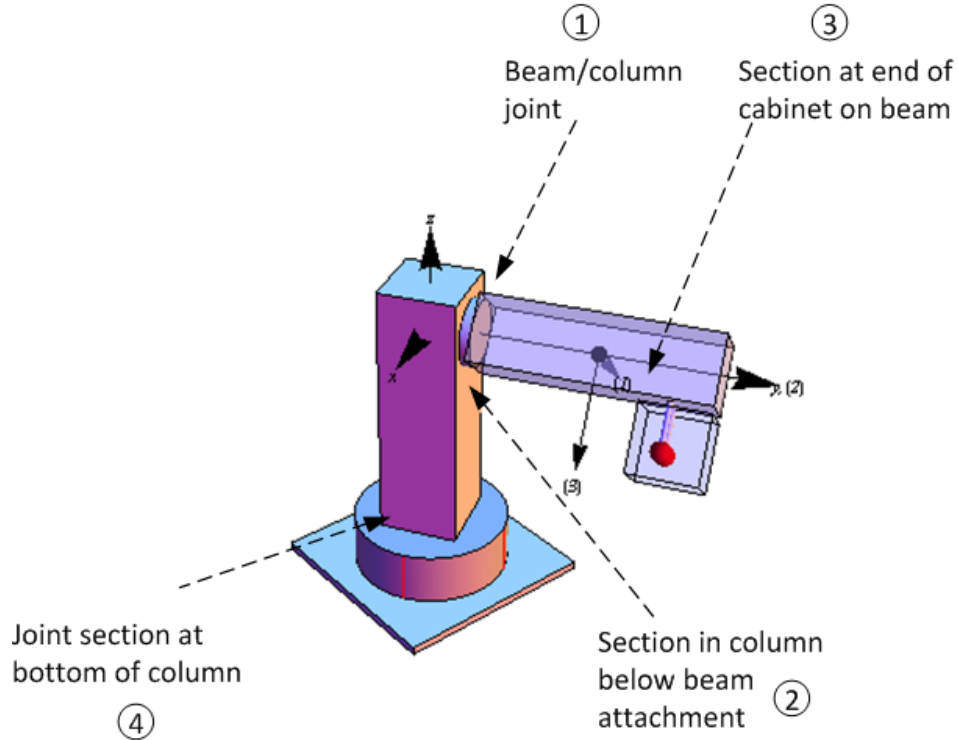
Figure 4: Identification of critical sections in the structure

simulation software due to time limitation to fully implement them in an acceptable manner. Due to also time limitations analysis for section 2 and 4 were not completed. The design team felt that protecting against failure in section 1 was the most important part at this design stage as this is the most likely failure section. If awarded the design, the team will include full analysis of all sections using finite element methods for most accurate results.

3 Mathematical model of system dynamics

This section explains and shows the derivation of the mathematical model and dynamic equations. These equations are used in the implementation of the software simulator in order to test and validate the design and select the final optimal design parameters.

3.1 Review of the model structure used in the design

There are two rigid bodies: the beam and the supporting column. The cabinet is part of the beam but was analyzed as a rigid body on its own in order to simplify the design by avoiding the determination of moments of inertia for a composite shaped body. The following architectural drawing shows the ride structure. The ride consists of the main support vertical column attached to a spinning base. Attached to one side of the column is an aluminum beam connected to the column using a drive shaft coupling that allow the beam to spin while attached to the column. A motor supplies the power needed to spin the shaft.

The cabinet is mounted and welded on the beam. The location of the cabinet on the beam is a configurable parameter in the design, and was adjusted during simulation to find an optimal location for the seating cabinet. In final design the cabinet was located at the far end of the beam to achieve maximum passenger felt acceleration.

The passengers are modeled as one rigid body of an equal side solid cube of a mass that represents the total mass of the passengers (maximum of 2 persons) with additional mass to account for the seating weight and a factor of safety. The factor of safety was also an adjustable parameter in the simulation. The following diagram shows the main dimensions of the structure used in the design.
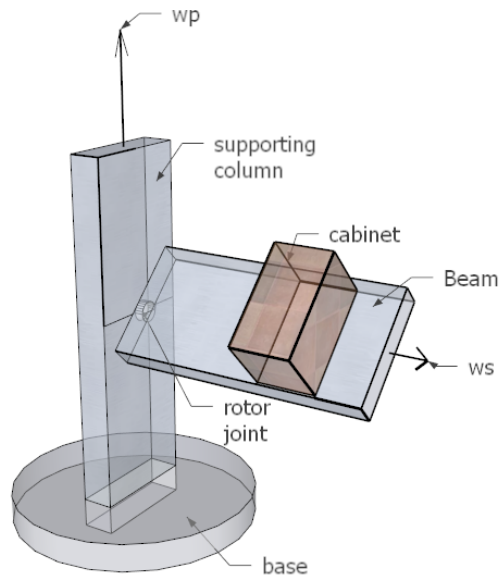
Figure 5: Main parts of the ride structure
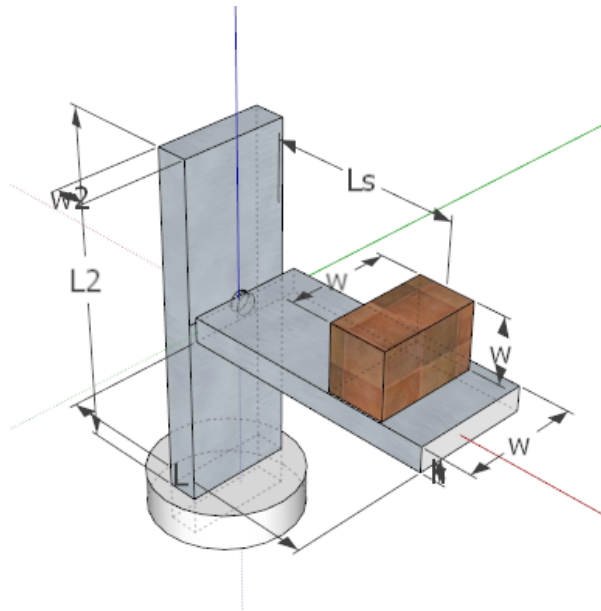
Figure 6: Main dimensions of ride structure

3.2   Setting up the mathematical model

Euler rigid body dynamic equations of motion are used to determine the dynamic moments due to the rotational motion of the rigid bodies. Principal Body axes, with its origin at the center of mass of each rigid body was used as the local body fixed coordinates system. Newton method is used to obtain the dynamics forces due to translation motion of the beam center of mass and also the center of mass of the cabinet. The column has rotational motion only and no translation motion.

After finding the dynamic forces, the unknown reaction forces at the joint between the beam and the column are solved for. Since these forces are functions of time, simulation was required to check that they remain below yield strength of Aluminium during the ride duration. Analytical solution is difficult due to the nonlinearity of the equations of motion, but a numerical solution of the equations of motion would

have been possible.

From beam bending moment diagrams generated for this design, the cross section at the beam/column joint was determined to be the critical section. This is the section which will have the maximum bending moment as well maximum shear force.

During simulation, the current values of the bending moment and shear force at the joint were tracked for each time step taken. The maximum values of these are used to determine the corresponding maximum stress concentration on the section to insure they do not reach 0.55 of yield strength of Aluminum. 0.55 was used to protect against failure in shear which can occur before failure in tension.

In order to minimize the number of parameters to vary in the design, the width of the cabinet was set to be the same as the beam width. The stresses in the beam are calculated based on simple beam theory and not plate theory. Due to time limitation, finite element analysis would was not performed. Finite element analysis would give more accurate stress calculations which would have allowed the design to be free to use less material by using thin plate for the platform and not thick beam as was used.

The following is a summary of the main steps used in the dynamic analysis process

1. Break the system into 3 separate rigid bodies

2. Use Euler and Newton methods to determine dynamic loads on each body. Principal body fixed axes are used with the reference point being the center of mass. (called case one analysis or $\omega = \Omega$).

3. Draw free body diagram for each body and balance the dynamic loading found in the above step in order to solve for unknown reaction forces.

4. Apply these reactions forces to the second rigid body connected to the first body by reversing the sign on all vector. These new vectors now act as external loads on the second rigid body.

5. Perform Euler and Newton analysis on the second body to find its dynamic loads needed to cause it motion.

6. Make free body diagram for the second body to balance the external forces with the dynamic loads and remembering to use the loads found in step 3 as external loads to this second body.

This diagram below illustrate the different coordinates axes used. The rotating coordinates system that all forces and resolved for is the xyz. This has its origin at the joint between the beam and the column. This coordinates system is attached to the column and rotates with the column at an absolute angular velocity ω_p. Each rigid body has its own local body fixed coordinates system $x'y'z'$. In this design, $x'y'z'$ have the origin at the center of mass of each rigid body and are aligned with the body principal axes. Hence $x'y'z'$ is the same as the e_1, e_2, e_3 axes commonly used to mean the principal axes. Therefore $\omega = \Omega$ in all cases. Once dynamic loads are found using $x'y'z'$ the results are transformed back to the xyz coordinates system. This way all the results from different rigid bodies are resolved with respect to a common coordinates system xyz (which is itself a rotating coordinates system).

Principal axes is the same as local body fixed coordinates system
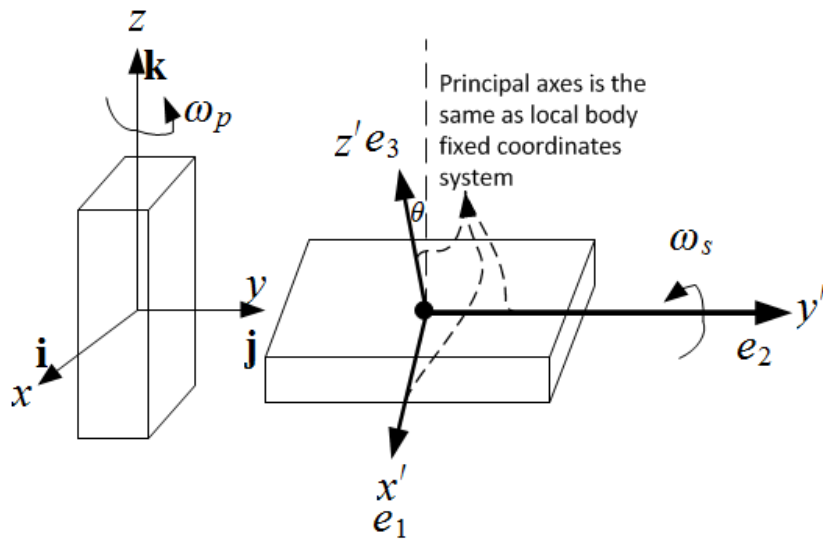
$$\boldsymbol{\Omega}_{body} = \omega_p \cos\theta \mathbf{e}_3 - \omega_p \sin\theta \mathbf{e}_1 + \omega_s \mathbf{e}_2$$

The body angular velocity is the same as its coordinates system angular velocity x'y'z' and is expressed as the body absolute angular velocity but using body fixed coordinates system

Figure 7: relation between rotating coordinates system, body fixed coordinates system, and body principal axes.

3.2.1 Summary of design input and design output

The following tables summarize the input and the output of the overall design. The tables list all the design parameters and the meaning and usage of each. They show what is known at the start of the design and the output from the design and simulation

Parameter name	Meaning and usage
ρ	Density of Aluminum 2700 $\frac{kg}{m^3}$, $E = 69$ GPa, Max tensile 125 MPa, Max yield strength 55 MPa
q	Mass per unit length of the beam
L	Length of the beam
L_s	Distance to the center of cabinet from the left edge of the beam
h	Thickness of the beam (rectangular cross section beam)
b	Width of the beam and cabinet
$\dot{\omega}_p$	Angular acceleration of vertical column (zero at steady state)
$\dot{\omega}_s$	Angular acceleration of platform and cabinet (zero at steady state)
m	Total mass of cabinet. 175 lbs per person, total of two persons including additional 200 lbs for seats
M	Mass of main support column. Fixed in design
$gLimit$	Maximum acceleration felt by rider. Must not exceed 6 g
σ_{yield}	Yield tensile stress for Aluminum. 55 MPa

Table 1: design input parameters

The following table shows the output of the design based on the above input. Simulation was used to find an optimal set of input parameters in order to achieve the customer specifications

Parameter name	Meaning and usage
$\mathbf{a}_m$	Acceleration time history experienced by passenger. Not to exceed $6g$
$\mathbf{F}_{weld}$	Reaction forces at joint connecting the beam with the column
$\mathbf{M}_{weld}$	Reaction moment at joint connecting the beam with the column
ω_p	Column angular velocity time history
ω_s	Beam angular velocity time history
σ	Direct stress tensor at critical section (joint between beam and column)
τ	Shear stress tensor at critical section (joint between beam and column)
$\sigma_{\max}$	Maximum direct stress recorded, must remain below yield stress for Aluminium
$\tau_{\max}$	Maximum shear stress recorded, must remain below 0.55 of tensile yield stress
$a_{\max}$	Maximum acceleration reached by riders. Must be as close as possible to $6g$
$v_{\max}$	Maximum velocity reached by riders. Typical value from simulation was 180 m.p.h.

Table 2: design output

3.2.2 System dynamic loads and free body diagram

Before starting the derivation, the following two diagrams are given to show the dynamic loads to be balanced with constraint forces. Two free body diagrams used. One for the beam and one for the column.
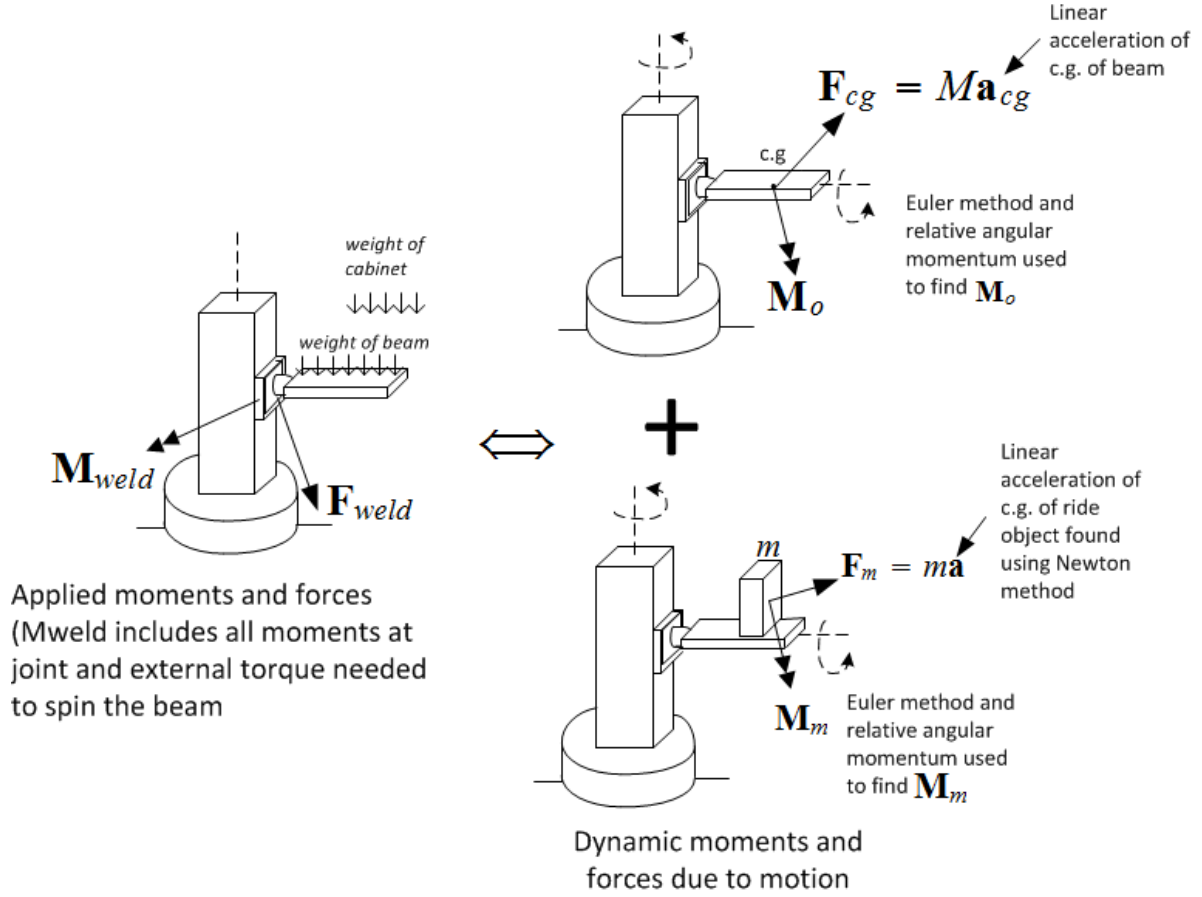
Figure 8: Beam dynamics. Balancing dynamic forces to external forces and reactions

After M_{weld} and F_{weld} are solved for, they are used (with negative signs) as known constraint forces on the column in order to solve for the column's own constraint forces and any external loads. The free body diagram for the column is given below The analysis below shows all five derivations. The first obtains $\mathbf{M}_{Beam}$ (dynamic moment to rotate the beam) using Euler method. The second finds $\mathbf{M}_{cabinet}$ (dynamic moment to rotate the cabinet) using Euler method, the third uses Newton method to find linear acceleration of center of mass $\mathbf{F}_{cabinet}$ (dynamic force to translate the cabinet), the fourth finds the linear acceleration of the center of the beam and $\mathbf{F}_{Beam}$ and the final derivation finds $\mathbf{M}_{column}$ (dynamic moment to rotate the column).

3.3 Beam to column analysis

3.3.1 Finding $\mathbf{M}_{beam}$ (beam dynamic moment)

The platform is modeled as a rectangular beam. Its principal moments of inertia are given below. Let $\boldsymbol{\omega}$ be the absolute angular velocity of the local body rotating coordinates $x'y'z'$. Let Ω be the beam (the body) absolute angular velocity. Hence

$$\boldsymbol{\omega}_{cs} = \omega_p \mathbf{k} + \omega_s \mathbf{j}$$

But $\boldsymbol{\omega}_{cs} = \boldsymbol{\Omega}_{body}$, therefore

$$\boldsymbol{\Omega}_{body} = \omega_p \mathbf{k} + \omega_s \mathbf{j}$$
$$\boldsymbol{\Omega}_{body} = \omega_p \cos\theta \mathbf{e}_3 - \omega_p \sin\theta \mathbf{e}_1 + \omega_s \mathbf{e}_2$$

Figure 9: Column dynamics. Balance with and external loads and beam transferred loads.

Figure 10: Configuration used for finding torque and force at beam/column joint
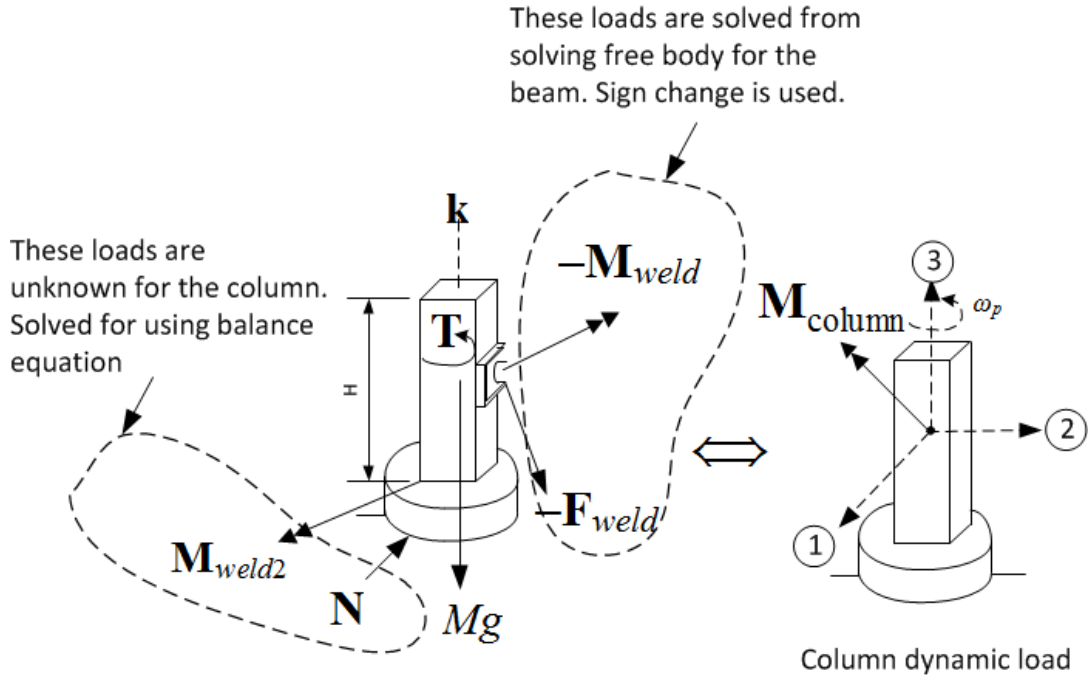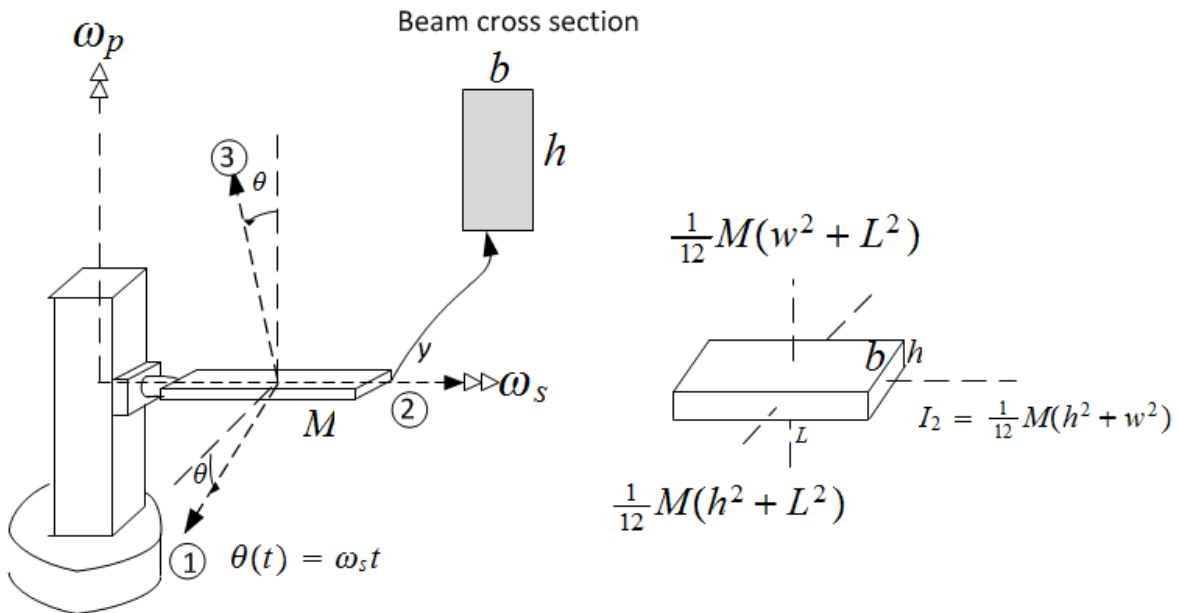
In component form

$$\Omega_1 = -\omega_p \sin\theta$$
$$\Omega_2 = \omega_s$$
$$\Omega_3 = \omega_p \cos\theta$$

Taking time derivative

$$\dot{\boldsymbol{\Omega}} = \left(\dot{\boldsymbol{\Omega}}\right)_r$$
$$= -\left(\dot{\omega}_p \sin\theta + \omega_p\omega_s \cos\theta\right)\mathbf{e}_1 + \dot{\omega}_s\mathbf{e}_2 + \left(\dot{\omega}_p \cos\theta - \omega_p\omega_s \sin\theta\right)\mathbf{e}_3$$

In component form

$$\dot{\Omega}_1 = -\dot{\omega}_p \sin\theta - \omega_p\omega_s \cos\theta$$
$$\dot{\Omega}_2 = \dot{\omega}_s$$
$$\dot{\Omega}_3 = \dot{\omega}_p \cos\theta - \omega_p\omega_s \sin\theta$$

The moments of inertia of the beam using its principal axes at the center or mass are

$$I_1 = \frac{1}{12}M\left(h^2 + L^2\right)$$
$$I_2 = \frac{1}{12}M\left(h^2 + b^2\right)$$
$$I_3 = \frac{1}{12}M\left(b^2 + L^2\right)$$

Since $\rho_c = 0$ (center of mass is used as reference point) then

$$M\rho_c \times \ddot{\mathbf{r}}_p = 0$$

Moments of inertia cross products are all zero since principal axes is used. The relative angular momentum of the beam becomes

$$\mathbf{h}_p = \begin{pmatrix} I_1 & 0 & 0 \\ 0 & I_2 & 0 \\ 0 & 0 & I_3 \end{pmatrix} \begin{pmatrix} \Omega_1 \\ \Omega_2 \\ \Omega_3 \end{pmatrix}$$

The rate of change of the relative angular momentum of the beam using Euler equations is

$$\dot{\mathbf{h}}_p = \begin{pmatrix} \dot{h}_1 \\ \dot{h}_2 \\ \dot{h}_3 \end{pmatrix} = \begin{pmatrix} I_1\dot{\Omega}_1 + \Omega_2\Omega_3\left(I_3 - I_2\right) \\ I_2\dot{\Omega}_2 + \Omega_1\Omega_3\left(I_1 - I_3\right) \\ I_3\dot{\Omega}_3 + \Omega_1\Omega_2\left(I_2 - I_1\right) \end{pmatrix}$$

Therefore, the moment needed to rotate the beam with the angular velocity specified is

$$\mathbf{M}_p = \dot{\mathbf{h}}_p$$

The above components are expressed using in the beam body fixed coordinates system $x'y'z'$ (which is the same as e_1, e_2, e_3 in this case). These are converted back to the xyz coordinates system using the following transformation

$$\mathbf{M}_x = \mathbf{M}_{p1}\cos\theta + \mathbf{M}_{p3}\sin\theta$$
$$\mathbf{M}_y = \mathbf{M}_{p2}$$
$$\mathbf{M}_z = -\mathbf{M}_{p1}\sin\theta + \mathbf{M}_{p3}\cos\theta$$

3.3.2 Finding $\mathbf{M}_{\text{col}}$ (column dynamic moment)

The main support column has one degree of freedom as it only spins around its z axes with angular velocity ω_p. Its center of mass does not translate in space. The column has a square cross section. Its height and sectional area were fixed in the design to allow changing the beam and cabinet parameters freely and see the effect on the joint stresses between the beam and the column as the failure point in the design was considered to be the the joint between the beam and the column This is a case of one body rotating around its own axes. Therefore,

$$\mathbf{M}_z = I_3\dot{\omega}_p$$

$$I_3 = \frac{1}{12}m_{col}(2r^2)$$
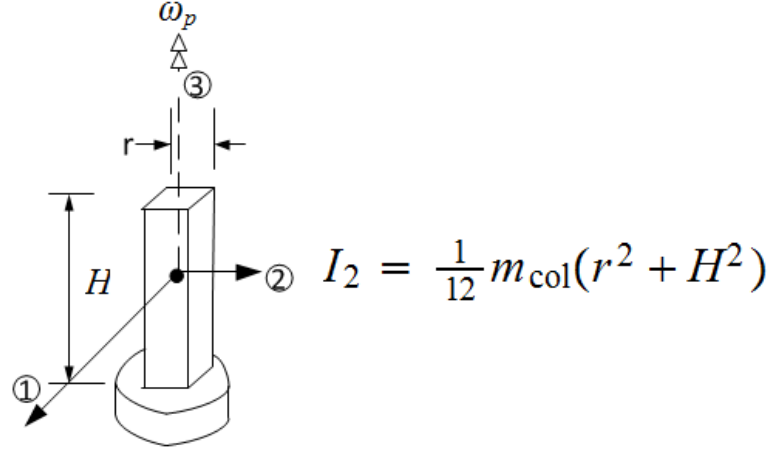
$$I_2 = \frac{1}{12}m_{col}(r^2 + H^2)$$

$$I_1 = \frac{1}{12}m_{col}(r^2 + H^2)$$

Where

$$I_3 = \frac{1}{12}m_{col}\left(2r^2\right)$$
$$= \frac{1}{6}m_{col}r^2$$

Where m_{col} is the mass of the column. Hence

$$M_{column} = \frac{1}{6}Mr^2\dot{\omega}_p$$

3.3.3 Finding $M_{cabinet}$ (cabinet dynamic moment)

The passengers including the cabinet are modeled as solid cube rigid body. The cabinet and the beam rotate with the same absolute angular velocity and act as one solid body. They were analyzed separately as it is easier to find the moment of inertias of each body separately than if both were combined.

The center of mass of the cabinet is at a distance $\frac{h}{2}$ above the beam where h is the width of cube which is the same as the beam width. Since the cabinet is attached to the platform and is a rigid body as well, the same exact analysis that was made to the beam above can be used for the cabinet. The only difference is that the moments of inertia I_1, I_2, I_3 are different. In this case they are

$$I_1 = I_2 = I_3 = \frac{1}{12}m\left(b^2 + h^2\right)$$

Therefore, the body dynamic moments are

$$\mathbf{M}_1 = I_1\dot{\Omega}_1 + \Omega_2\Omega_3\left(I_3 - I_2\right)$$
$$\mathbf{M}_2 = I_2\dot{\Omega}_2 + \Omega_1\Omega_3\left(I_1 - I_3\right)$$
$$\mathbf{M}_3 = I_1\dot{\Omega}_1 + \Omega_2\Omega_3\left(I_3 - I_2\right)$$

The above components are expressed using the cabinet own principal axes coordinates system $x'y'z'$ (local body coordinate systems) which is its principal axes in this case. These are converted back to the xyz coordinates using the same transformation used for the beam

$$\mathbf{M}_x = \mathbf{M}_1\cos\theta + \mathbf{M}_3\sin\theta$$
$$\mathbf{M}_y = \mathbf{M}_2$$
$$\mathbf{M}_z = -\mathbf{M}_1\sin\theta + \mathbf{M}_3\cos\theta$$
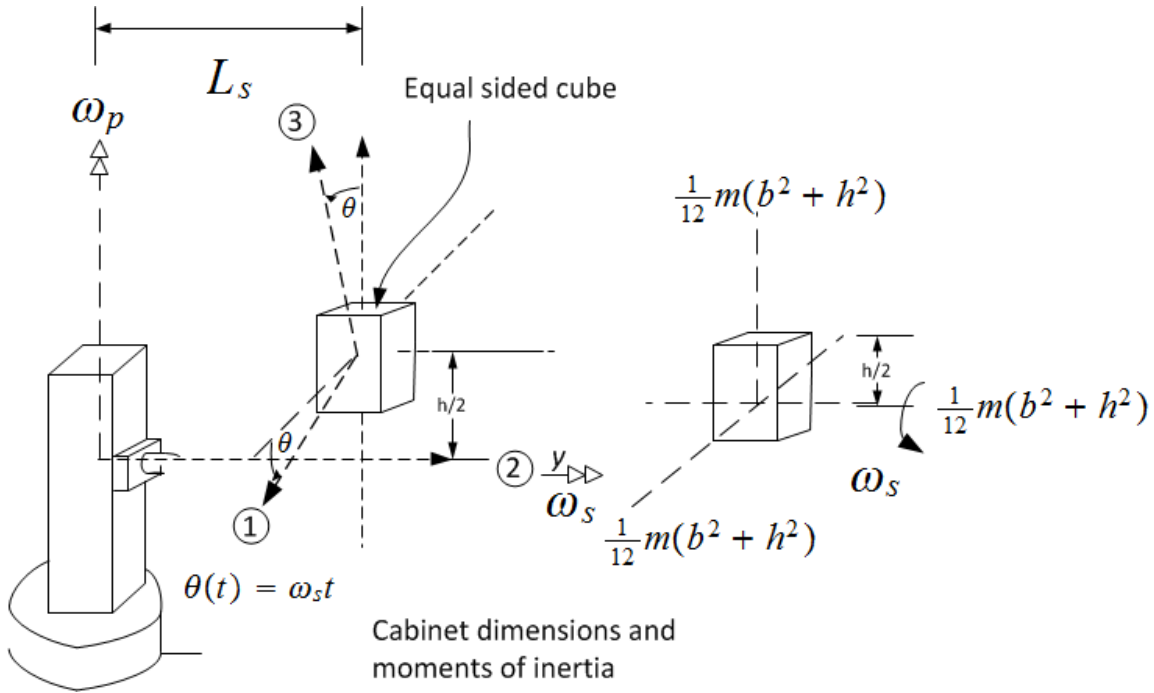
3.3.4 Finding $\mathbf{F}_{cabinet}$ (cabinet dynamic linear force)

To find $\mathbf{F}_m = m\mathbf{a}$ for the cabinet, Newton method is used as follows The rotating coordinates system xyz
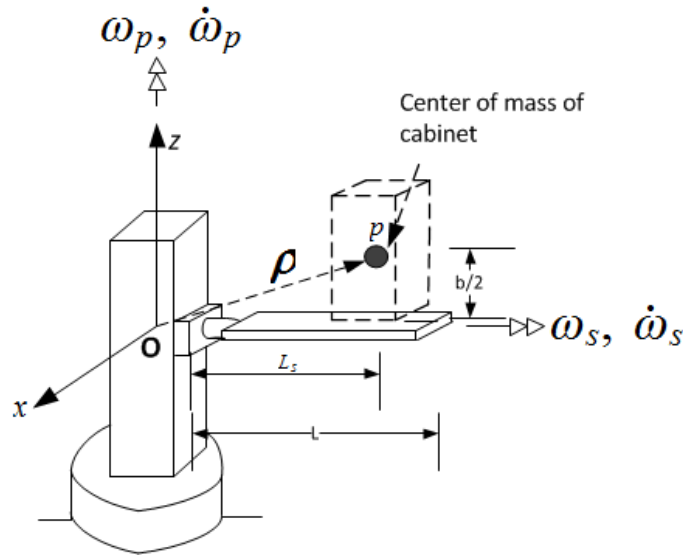
Figure 11: Rotating coordinates system xyz used to find passenger acceleration

has its origin at the beam column joint. xyz is attached to the column and rotates with the column with angular velocity $\omega_p\mathbf{k}$. The center of mass of the cabinet shown above as the circle p, is at distance L_s from the origin O.

All calculations are expressed using unit vectors of the rotating coordinates system and are valid for all time. In the rotating coordinates system, point p, the center of mass of cabinet, appears as shown in the following diagram. In this diagram θ is the angle p makes with the z axes, where $\theta = \omega_s t$ and $\dot{\theta} = \omega_s$ Using the above diagrams, the absolute velocity of p is found as follows

Figure 12: View of passenger head in the rotating coordinates system xyz

$$\boldsymbol{\rho} = L_s\mathbf{j} + \frac{b}{2}\sin\theta\mathbf{i} + \frac{b}{2}\cos\theta\mathbf{k}$$

$$\dot{\boldsymbol{\rho}}_r = \frac{b}{2}\omega_s\cos\theta\mathbf{i} - \frac{b}{2}\omega_s\sin\theta\mathbf{k}$$

$$\dot{\mathbf{R}} = 0$$

$$\boldsymbol{\omega} = \omega_p\mathbf{k}$$

$$\boldsymbol{\omega} \times \boldsymbol{\rho} = -\omega_p L_s\mathbf{i} + \omega_p\frac{b}{2}\sin\theta\mathbf{j}$$

Hence the absolute velocity of p is

$$\mathbf{V} = \dot{\mathbf{R}} + \dot{\boldsymbol{\rho}}_r + \boldsymbol{\omega} \times \boldsymbol{\rho}$$

$$= \left(\frac{b}{2}\omega_s\cos\theta\mathbf{i} - \frac{b}{2}\omega_s\sin\theta\mathbf{k}\right) - \omega_p L_s\mathbf{i} + \omega_p\frac{b}{2}\sin\theta\mathbf{j}$$

$$= \left(\frac{b}{2}\omega_s\cos\theta - \omega_p L_s\right)\mathbf{i} + \omega_p\frac{b}{2}\sin\theta\mathbf{j} - \frac{b}{2}\omega_s\sin\theta\mathbf{k}$$

The absolute acceleration of p is found from

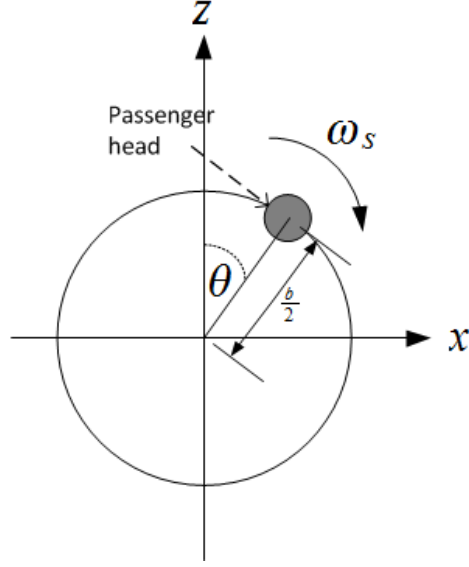$$\ddot{\boldsymbol{\rho}}_r = \left(\frac{b}{2}\dot{\omega}_s\cos\theta - \frac{b}{2}\omega_s^2\sin\theta\right)\mathbf{i} - \left(\frac{b}{2}\dot{\omega}_s\sin\theta + \frac{b}{2}\omega_s^2\cos\theta\right)\mathbf{k}$$

$$\ddot{\mathbf{R}} = 0$$

$$\dot{\boldsymbol{\omega}} = \dot{\omega}_p\mathbf{k}$$

$$\boldsymbol{\omega} \times (\boldsymbol{\omega} \times \boldsymbol{\rho}) = \omega_p\mathbf{k} \times \left(-\omega_p L_s\mathbf{i} + \omega_p\frac{b}{2}\sin\theta\mathbf{j}\right) = -\omega_p^2 L_s\mathbf{j} - \omega_p^2\frac{b}{2}\sin\theta\mathbf{i}$$

$$\boldsymbol{\omega} \times \dot{\boldsymbol{\rho}}_r = \omega_p\mathbf{k} \times \left(\frac{b}{2}\omega_s\cos\theta\mathbf{i} - \frac{b}{2}\omega_s\sin\theta\mathbf{k}\right) = \frac{b}{2}\omega_p\omega_s\cos\theta\mathbf{j}$$

$$\dot{\boldsymbol{\omega}} \times \boldsymbol{\rho} = \dot{\omega}_p\mathbf{k} \times \left(L_s\mathbf{j} + \frac{b}{2}\sin\theta\mathbf{i} + \frac{b}{2}\cos\theta\mathbf{k}\right) = -\dot{\omega}_p L_s\mathbf{i} + \dot{\omega}_p\frac{b}{2}\sin\theta\mathbf{j}$$

Therefore the absolute acceleration of the passenger is

$$\mathbf{a} = \ddot{\mathbf{R}} + \ddot{\boldsymbol{\rho}}_r + 2\left(\boldsymbol{\omega} \times \dot{\boldsymbol{\rho}}_r\right) + \left(\dot{\boldsymbol{\omega}} \times \boldsymbol{\rho}\right) + \boldsymbol{\omega} \times \left(\boldsymbol{\omega} \times \boldsymbol{\rho}\right)$$

$$= \left(\frac{b}{2}\dot{\omega}_s \cos\theta - \frac{b}{2}\omega_s^2 \sin\theta\right)\mathbf{i} - \left(\frac{b}{2}\dot{\omega}_s \sin\theta + \frac{b}{2}\omega_s^2 \cos\theta\right)\mathbf{k}$$

$$+ \left(2\frac{b}{2}\omega_p\omega_s \cos\theta\mathbf{j}\right) + \left(-\dot{\omega}_p L_s\mathbf{i} + \dot{\omega}_p\frac{b}{2}\sin\theta\mathbf{j}\right) - \left(\omega_p^2 L_s\mathbf{j} + \omega_p^2\frac{b}{2}\sin\theta\mathbf{i}\right)$$

Simplifying gives

$$\mathbf{F}_{cabinet} = m\mathbf{a}$$

$$= \mathbf{i}\left(\frac{b}{2}\dot{\omega}_s \cos\theta - \frac{b}{2}\omega_s^2 \sin\theta - \dot{\omega}_p L_s - \omega_p^2\frac{b}{2}\sin\theta\right)m$$

$$+ \mathbf{j}\left(b\omega_p\omega_s \cos\theta + \dot{\omega}_p\frac{b}{2}\sin\theta - \omega_p^2 L_s\right)m$$

$$- \mathbf{k}\left(\frac{b}{2}\dot{\omega}_s \sin\theta + \frac{b}{2}\omega_s^2 \cos\theta\right)m$$

The above is expressed using the common xyz rotating coordinate system

3.3.5   Finding $\mathbf{F}_{beam}$ (beam dynamic translational force)

The linear acceleration of the center of mass of platform, which is located at distance $\frac{L}{2}$ from the origin o of the xyz rotating coordinates system.   Therefore
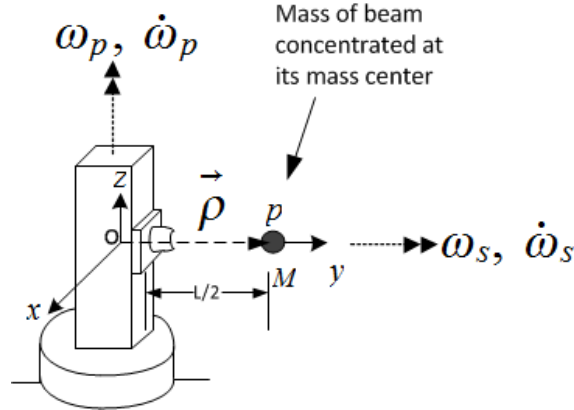
Figure 13: Rotating coordinates system xyz used to find beam center of mass acceleration

$$\boldsymbol{\rho} = \frac{L}{2}\mathbf{j}$$

$$\boldsymbol{\omega} = \omega_p\mathbf{k}$$

$$\boldsymbol{\omega} \times \boldsymbol{\rho} = -\omega_p\frac{L}{2}\mathbf{i}$$

$$\dot{\boldsymbol{\rho}}_r = 0$$

$$\dot{\mathbf{R}} = 0$$

$$\dot{\boldsymbol{\omega}} = \dot{\omega}_p\mathbf{k}$$

$$\dot{\boldsymbol{\omega}} \times \boldsymbol{\rho} = \dot{\omega}_p\mathbf{k} \times \frac{L}{2}\mathbf{j} = -\dot{\omega}_p\frac{L}{2}\mathbf{i}$$

$$\boldsymbol{\omega} \times \left(\boldsymbol{\omega} \times \boldsymbol{\rho}\right) = \omega_p\mathbf{k} \times \left(-\omega_p\frac{L}{2}\mathbf{i}\right) = -\omega_p^2\frac{L}{2}\mathbf{j}$$

Hence

$$\mathbf{a}_{cg} = \ddot{\mathbf{R}} + \ddot{\boldsymbol{\rho}}_r + 2\left(\boldsymbol{\omega} \times \dot{\boldsymbol{\rho}}_r\right) + \left(\dot{\boldsymbol{\omega}} \times \boldsymbol{\rho}\right) + \boldsymbol{\omega} \times \left(\boldsymbol{\omega} \times \boldsymbol{\rho}\right)$$

$$= -\dot{\omega}_p \frac{L}{2}\mathbf{i} - \omega_p^2 \frac{L}{2}\mathbf{j}$$

Therefore

$$\mathbf{F}_{beam} = M\mathbf{a}_{cg}$$

$$= -M\frac{L}{2}\dot{\omega}_p \mathbf{i} - M\frac{L}{2}\omega_p^2 \mathbf{j}$$

The above is expressed using the xyz rotating coordinates system.

3.3.6 Using free body diagram and solving for constraint forces

The dynamic forces have been found from above. The are balanced with constraint forces and any external loads using free body diagram. The following diagram shows the balance between dynamic forces and moments and external forces. $\mathbf{M}_{weld}$ below is used to represent all constraint moments at the joint between the beam the column, including the extra torque needed to rotate the beam Taking moments at

External moments and forces needed to balance dynamic loads

Dynamic moments and forces due to motion

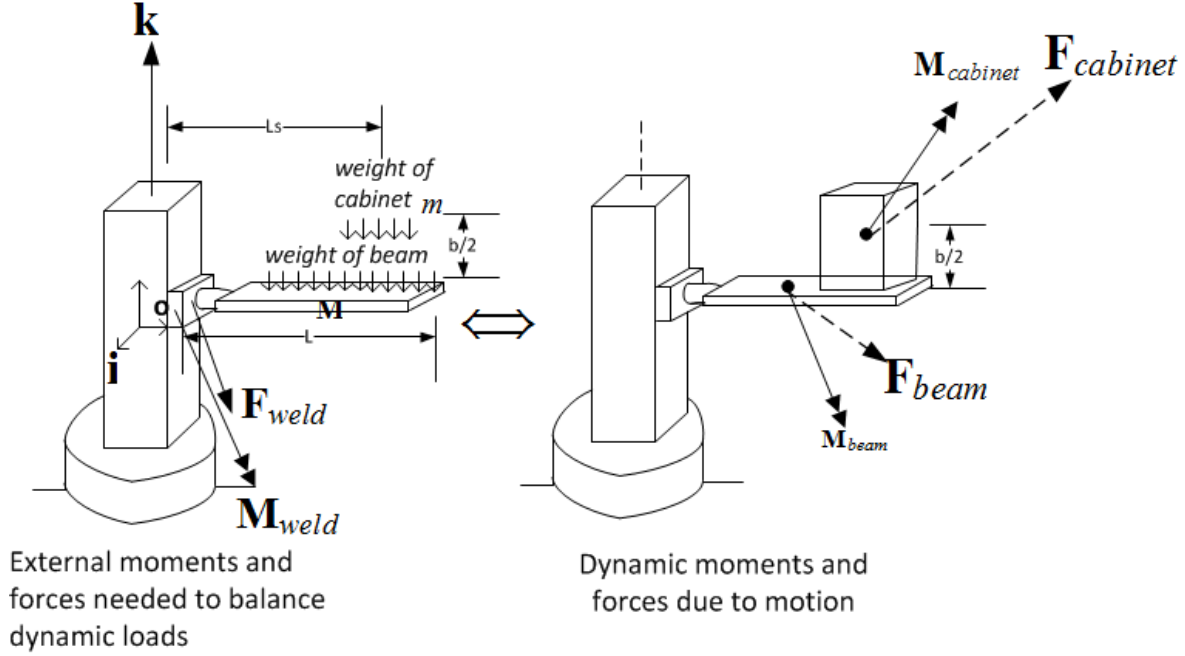point o, the left end of the beam which is the origin of the rotating coordinates system xyz

$$\mathbf{M}_{weld} + \left(\frac{L}{2}\mathbf{j} \times -Mg\mathbf{k}\right) + \left((L_s\mathbf{j}+\frac{b}{2}\mathbf{k}) \times -mg\mathbf{k}\right) = \mathbf{M}_{beam} + \mathbf{M}_{cabinet} + \left(\frac{L}{2}\mathbf{j} \times \mathbf{F}_{beam}\right) + \left(L_s\mathbf{j}+\frac{b}{2}\mathbf{k}\right) \times \mathbf{F}_{cabinet}$$

$$\mathbf{M}_{weld} - \frac{L}{2}Mg\mathbf{i} - L_smg\mathbf{i} = \mathbf{M}_{beam} + \mathbf{M}_{cabinet} + \left(\frac{L}{2}\mathbf{j} \times \mathbf{F}_{beam}\right) + \left(L_s\mathbf{j}+\frac{b}{2}\mathbf{k}\right) \times \mathbf{F}_{cabinet}$$

Hence

$$\mathbf{M}_{weld} = \left(\frac{L}{2}Mg + L_smg\right)\mathbf{i} + \mathbf{M}_{beam} + \mathbf{M}_{cabinet} + \left(\frac{L}{2}\mathbf{j} \times \mathbf{F}_{beam}\right) + \left(L_s\mathbf{j} + \frac{\mathbf{b}}{2}\mathbf{k}\right) \times \mathbf{F}_{cabinet}$$

The force vector at the joint is

$$\mathbf{F}_{weld} - Mg\mathbf{k} - mg\mathbf{k} = \mathbf{F}_{beam} + \mathbf{F}_{cabinet}$$

$$\mathbf{F}_{weld} = (Mg + mg)\mathbf{k} + \mathbf{F}_{beam} + \mathbf{F}_{cabinet}$$

19

Bending moment and shear force calculations Now that the constraint forces are solved for from the above analysis, the bending moment and shear force diagram are formulated. The moments will be a function of distance from the beam/column joint.

Let $\mathbf{BM}(\xi)$ be the moments vector at distance ξ along the beam length. There will be 3 components to this moment. Bending M_x, torsional M_y and twisting M_z. Let the weight be per unit length of the
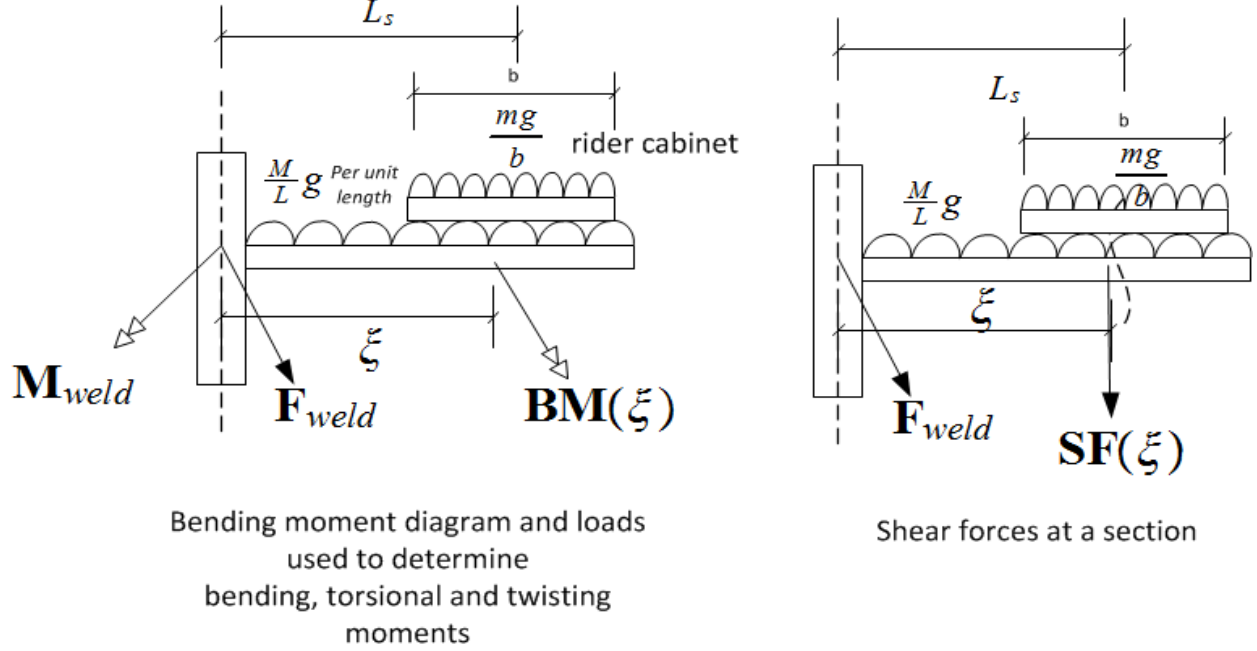

Figure 14: Finding the bending moment at different locations along the span of the beam

beam which is $\frac{M}{L}g$ be q. In the following, the notation $\langle \xi - x \rangle$ is used to indicate that the term is effective only when $\langle \xi - x \rangle$ is positive. Let the distance to start of the cabinet be

$$\alpha = L_s - \frac{b}{2}$$

Where b is the width of the cabinet.

$$\mathbf{BM}(\xi) = \mathbf{M}_{weld} + (\xi \mathbf{j} \times \mathbf{F}_{weld}) + \left(\frac{\xi}{2}\mathbf{j} \times -q\xi\mathbf{k}\right) + \left(\frac{\xi - \alpha}{2}\mathbf{j} \times -\frac{mg}{b}(\xi - \alpha)\mathbf{k}\right)\langle \xi - \alpha \rangle$$

In component form, the bending moment will be $\mathbf{BM}_x(\xi)$ and The torsion moment will be $\mathbf{BM}_y(\xi)$ and the twisting moment will be $\mathbf{BM}_z(\xi)$.

Let $\mathbf{SF}(\xi)$ be the shear force vector at distance ξ. Hence

$$\mathbf{SF}(\xi) = \mathbf{F}_{weld} - q\xi\mathbf{k} - \frac{mg}{b}(\xi - \alpha)\langle \xi - \alpha \rangle\mathbf{K}$$

The above completes the mathematical derivation of the dynamics of the system. The next step is to implement this model and use simulation to validate it and design for an optimal set of parameters.

Finding shear and direct stress from bending and shear forces The result of the above calculations is the moments and forces at the joint between the beam and the column and using $\mathbf{BM}(\xi)$ and $\mathbf{SF}(\xi)$ at any other section in the beam.

The next step is to use these to obtain complete description of stress state at the section. Due to lack of time finite element analysis was not performed. Therefore, basic beam theory equations were used for stress calculation. Care was taken to insure that the beam cross section selected had thickness not less that its width. Having a thin beam would require analysis using plate theory making it much more complicated. The disadvantages of this method is that the beam was much heavier than needed if thin beam was used, but the advantage is that the stress equations used are known to be valid in this case.

20

Given the moments M_x, M_y, M_z and the forces F_x, F_y, F_z all the cross section, the following equations were used. These equations assume a rectangle beam cross section of thickness h and width b and that $h \geq b$

$$\sigma_{\max} = \frac{M_x c}{I_{area}} = \frac{M_x \frac{h}{2}}{\frac{1}{12} bh^3}$$

$$\tau_{\max} = \frac{3V_{\max}}{2A}$$

Torsional stress was not fully developed in this design since it is a rectangular cross section and would require finite element analysis. The beam is expected to fail due to bending moment M_x and this is what the rest of the analysis address. Future analysis of stress concentration will use finite element analysis and will take torsion stress into account.

3.4   Column dynamic analysis

In the above section the constraint forces in the beam/column joints were found. These are now used as external forces on the column with an opposite sign. Free body diagram is used for the column in order to find the constraint forces and external loads acting on the column. The following diagram shows the free body diagram used
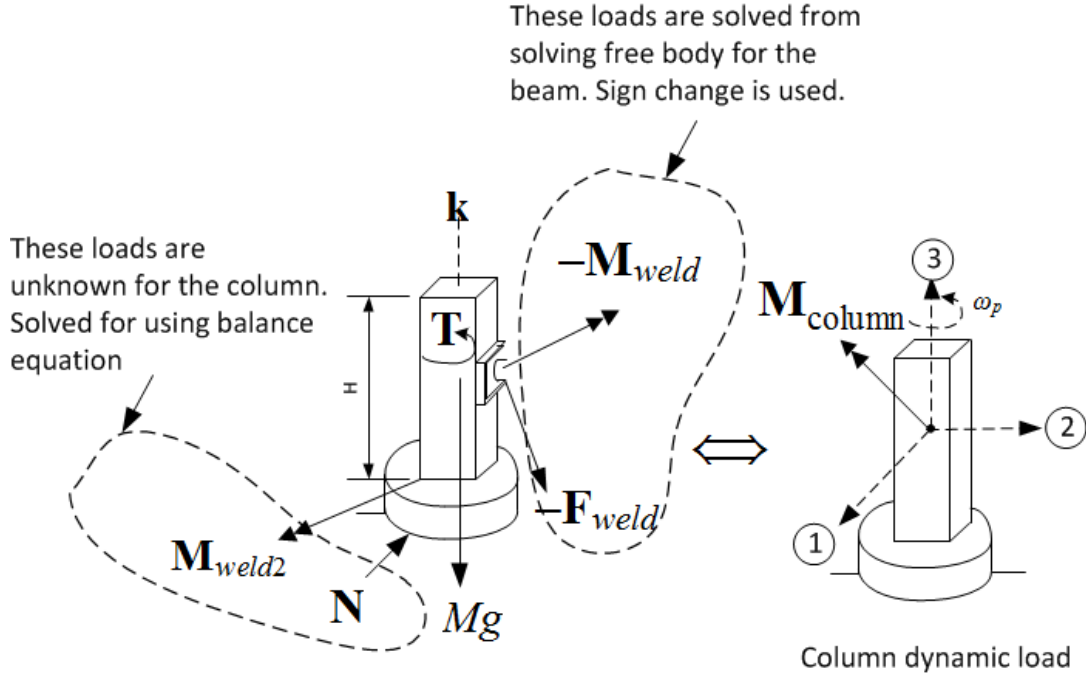
Figure 15: Dynamic load balance between column and external loads

Taking moments at the joint between the column and the ground

$$\mathbf{T} + \mathbf{M}_{weld2} - \mathbf{M}_{weld} + \left(-\frac{H}{2}\mathbf{k} \times -\mathbf{F}_{weld} \right) = \mathbf{M}_{\text{column}}$$

Solving for the unknown constraint force $\mathbf{N}$ and the external torque $\mathbf{T}$

$$\mathbf{M}_{weld2} + \mathbf{T} = \mathbf{M}_{\text{column}} - \left(\frac{H}{2}\mathbf{k} \times \mathbf{F}_{weld} \right) + \mathbf{M}_{weld}$$

The torque $\mathbf{T}$ is unknown at this stage and has to be determined by other means to obtain complete solution. This is the external torque needed to accelerate the column during ramp up and to decelerate it during ramp down phases. Combining all the unknowns into one term called $\mathbf{M}_{weld3}$, the above reduces to

$$\mathbf{M}_{weld3} = \mathbf{M}_{\text{column}} - \left(\frac{H}{2}\mathbf{k} \times \mathbf{F}_{weld} \right) + \mathbf{M}_{weld}$$

The balance equation for forces gives

$$\mathbf{N} - Mg\mathbf{k} - \mathbf{F}_{weld} = 0$$

$$\mathbf{N} = Mg\mathbf{k} + \mathbf{F}_{weld}$$

Now that all loads acting on the column are found, bending moment and shear force diagrams can be also be made or finite element analysis used in order to determine the stress state inside the column at every section.

4 Simulation of the dynamic equations found

4.1 Review of the simulation

The simulation accepts as input all the parameters shown in table 1 on page 11. The goal of the simulation is to verify visually the dynamics and to allow the selection of correct sizes for the structure and to insure that the acceleration does not exceed $6g$ using the selected parameters. Based on the simulation, one optimal set of values was selected and given in the conclusion section. The simulator displays tables showing all the current values for stress and moments found at the beam/column joint. It keeps track of the maximum stress values reached and uses these to determine the maximum stress using the equations shown above.

This diagram shows an overview of the user interface. This software can be run from the project web site located at `http://12000.org/my_notes/mma_demos/EMA542_project/index.htm`
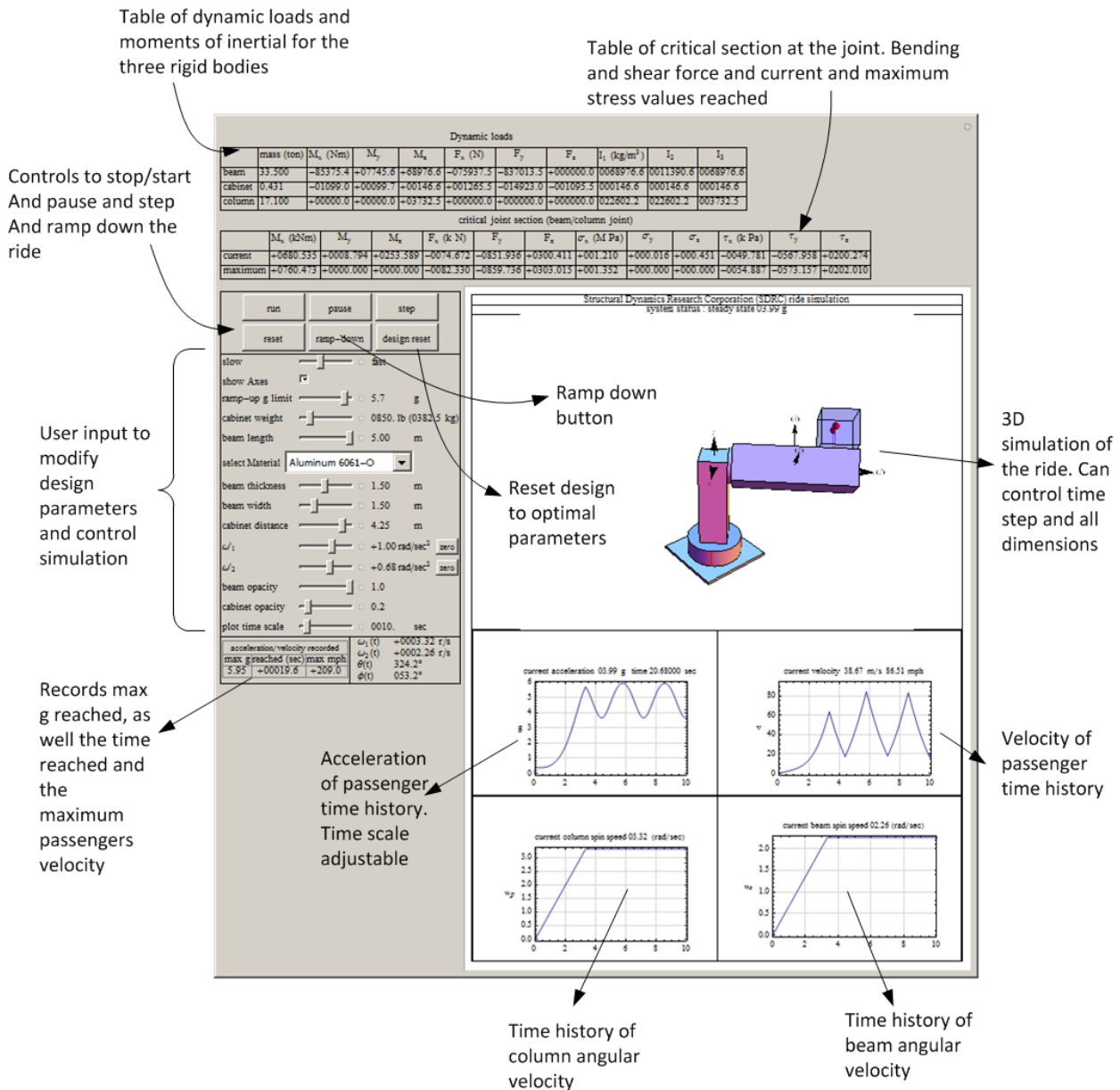

Figure 16: overview of simulator user interface

4.2 Simulation output, time histories and discussion of results

All these tables and results below are generated from the final design using the selected final optimal parameters.

Dynamic loads

	mass (ton)	M_x (Nm)	M_y	M_z	F_x (N)	F_y	F_z	I_1 (kg/m^3)	I_2	I_3
beam	10.400	−32963.4	+01417.5	+02086.9	−003307.5	−076914.6	+000000.0	0010434.4	0001575.0	0010434.4
cabinet	0.279	−00882.5	+00038.0	+00008.4	−000616.9	+001760.5	−011906.4	000042.2	000042.2	000042.2
column	17.100	+00000.0	+00000.0	+00746.5	+000000.0	+000000.0	+000000.0	022602.2	022602.2	003732.5

Figure 17: dynamic loads at the end of ride using optimal design values

critical joint section (beam/column joint)

	M_x (kNm)	M_y	M_z	F_x (k N)	F_y	F_z	σ_x (M Pa)	σ_y	σ_z	τ_x (k Pa)	τ_y	τ_z
current	+0099.060	+0001.147	+0009.734	−0003.924	−0075.154	+0083.183	+000.594	+000.007	+000.058	−0005.887	−0112.731	+0124.774
maximum	+0175.814	+0007.630	+0009.734	−0015.955	−0085.740	+0107.003	+001.055	+000.046	+000.058	−0023.932	−0128.610	+0160.505

Maximum direct stress was due to pending moment. Remained Well below the yield stress for Aluminum

Figure 18: critical section current and maximum moments and stresses

Guard limit found by trial used to stop the acceleration at. (passenger acceleration will reach the 6g using this but not exceed)

ramp−up g limit	5.8	g
cabinet weight	0550.1b (0247.5 kg)	
beam length	3.50	m
select Material	Aluminum 6061−O	
beam thickness	1.00	m
beam width	1.00	m
cabinet distance	3.00	m
ω'_1	+0.20 rad/sec^2	zero
ω'_2	+0.90 rad/sec^2	zero

Optimal parameters found by simulation

Figure 19: optimal set of parameters obtained from simulation.

acceleration/velocity recorded		
max g	reached (sec)	max mph
5.98	+00012.1	+187.0

Figure 20: simulator keeps track of maximum g felt by passenger to insure it does not exceed $6g$

First 15 seconds of time history of passenger acceleration data

Due to dynamics of motion, fluctuation of value of acceleration remain in steady state

First 15 seconds of time history of passenger velocity data

current acceleration 04.86 g   time 13.12000 sec

current velocity 75.07 m/s 167.90 mph

current column spin speed 02.16 (rad/sec)

current beam spin speed 09.70 (rad/sec)

Showing column angular velocity profile, showing steady increase then it reaches steady state

Steady state

Showing beam angular velocity profile, showing steady increase then it reaches steady state

Figure 21: acceleration and velocity of passenger time history and angular velocity time history of beam and column

6g reached, 5 second

Ramp down

ramp up

Velocity profile

Ramp down

ramp up

current acceleration 00.98 g time 24.14900 sec

current velocity 33.88 m/s 75.80 mph

current column spin speed 00.00 (rad/sec)

current beam spin speed 00.00 (rad/sec)
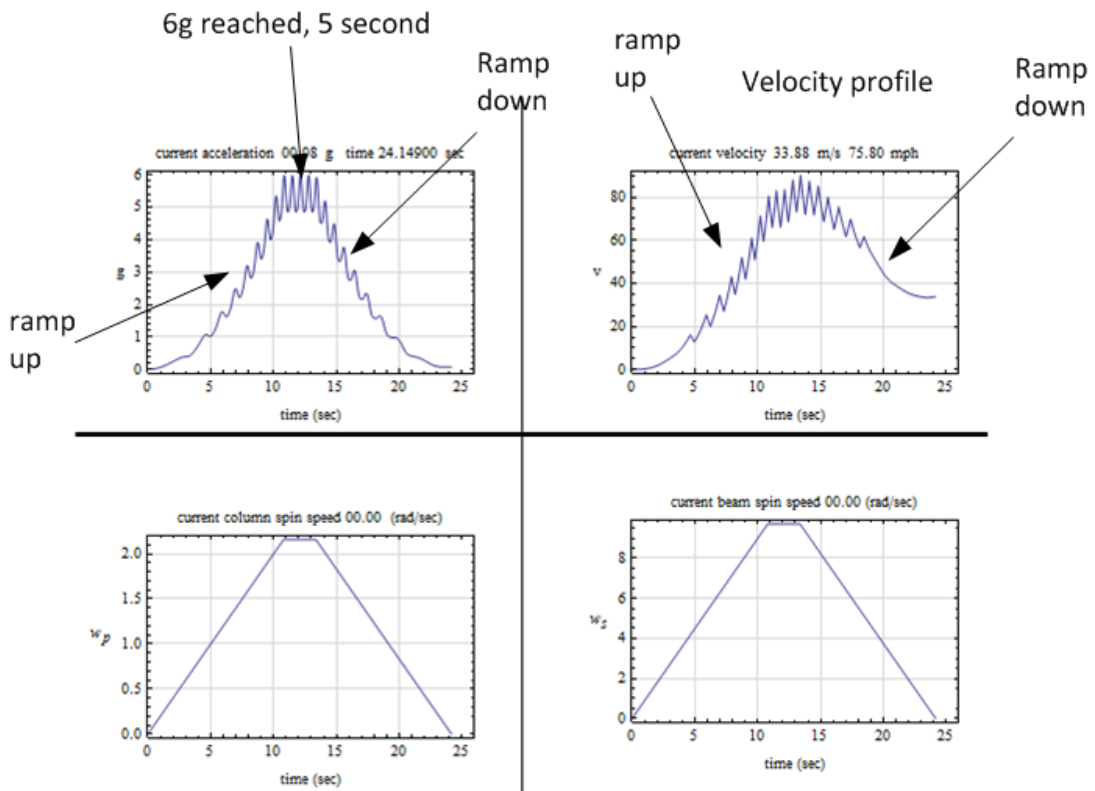
Column and beam angular velocities time histories shown effect of ramp down

Figure 22: time histories using the ramp down option used after reaching 6g goal

4.3 Discussion and analysis of results

The following table gives the optimal design parameters found by simulation of the derived model in order to achieve the customer requirements.

parameter	value	description
beam mass	10.4 ton	one ton is 2000 lbs
beam width	1 meters	
beam thickness	1 meters	
beam length	3.5 meters	
cabinet mass	560 lbs	includes 2 passengers, seating, frame and factor of safety
cabinet height	1 meters	
cabinet width	1 meters	
column mass	17.1 ton	
column cross section	3 by 3 meters	
maximum bending moment M_x	175 KNm	
maximum torsion moment M_y	7.6 KNm	
maximum twisting moment M_z	28 KNm	
maximum shear force F_x	-15.96 KN	
maximum shear force F_y	-85 KN	
maximum shear force F_z	107 KN	
maximum direct stress σ_x	1.055 MPa	Below tensile yield. Pure Aluminium has 10 MPa. and
maximum direct stress σ_y	0.046 MPa	Aluminium 6061-O yields at 200 MPa.
maximum direct stress σ_z	0.172 MPa	
maximum shear stress τ_x	-23.94 KPa	
maximum shear stress τ_y	-128.6 KPa	
maximum shear stress τ_z	150.5 KPa	

Table 3: design output for loading and forces using optimal parameters found

It was found that in order to be able to achieve the $6g$ limit and not exceed it, the acceleration have to put turned off well before the $6g$ is detected. This can be seen by examining the passenger acceleration expression from above, which is

$$\mathbf{a} = \mathbf{i}\left(\frac{b}{2}\dot{\omega}_s\cos\theta - \frac{b}{2}\omega_s^2\sin\theta - \dot{\omega}_p L_s - \omega_p^2\frac{b}{2}\sin\theta\right)$$

$$+\mathbf{j}\left(2\frac{b}{2}\omega_p\omega_s\cos\theta + \dot{\omega}_p\frac{b}{2}\sin\theta - \omega_p^2 L_s\right)$$

$$+\mathbf{k}\left(-\frac{b}{2}\dot{\omega}_s\sin\theta - \frac{b}{2}\omega_s^2\cos\theta\right)$$

We can see that, by letting $\dot{\omega}_s$ and $\dot{\omega}_p$ then the acceleration becomes

$$\mathbf{a} = \mathbf{i}\left(-\frac{b}{2}\omega_s^2\sin\theta - \omega_p^2\frac{b}{2}\sin\theta\right) + \mathbf{j}\left(2\frac{b}{2}\omega_p\omega_s\cos\theta - \omega_p^2 L_s\right) - \mathbf{k}\frac{b}{2}\omega_s^2\cos\theta$$

Even though from now on the angular velocities ω_s and ω_p are constant, this does not imply that $\mathbf{a}$ will become constant. Since θ is still changing in time, then $\mathbf{a}$ will still fluctuate in periodic fashion from now on. Hence the passenger acceleration can still exceed $6g$ if we were to turn off the ramp up acceleration too close to $6g$. For this reason the value the acceleration was turned off at $5.8g$ in order to final value of $5.98g$ as felt by the passengers.

4.4   Cost analysis

Based on the above result and using the mass needed, the following table gives a summary of cost for construction of the ride
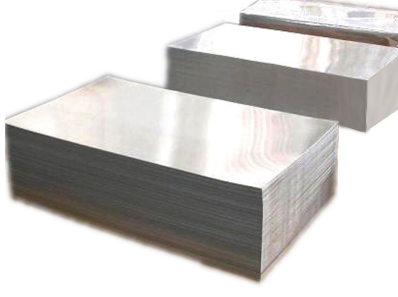
item	cost	description
cost of Aluminum alloy 6061-O	$0.8 per lb.	can depend on market conditions
beam material cost (10.4 ton)	$16,000	$(10.4)(2000)(0.8)$
column material cost (17.1 ton)	$27,360	$(17.1)(2000)(0.8)$
cabinet material cost (500 lb.)	$446.5	
Labor cost for construction	$12,000	300 labor hrs @ 40 per hr.
Equipment and labor insurance	$10,000	
Management cost (one manager)	$4,000	50 hrs @ $80 per hr.
Electric spindel motors for column and beam	$10,000	2 @ $5,000
Total cost	**$79,806**	

Table 4: cost estimate

The major part of the cost is for material. This is due to the use of thick beam and column. This allowed the use of basic beam theory stress analysis. This cost however can be reduced by the use of plate theory or numerical finite elements methods in order to be able to safely used less material and reduce the thickness of the beam and column while insuring accurate stress calculations.

5 Conclusions of results and future work

The final design given above meets the requirement specification that the customer provided. Using simulation, it was possible to validate the equations found and to confirm that the beam/column section is safe for the selected optimal parameters.

The selected parameters allow the passengers to reach almost $6g$ in 12 seconds using a ride that consist of two noncollinear angular velocities. There are many different profiles that could have been selected to achieve this goal. The set selected reached the closest to $6g$ without crossing over and that is why it was selected. The following is the final design used

parameter	value	description
maximum g reached	5.98 **g**	After many simulations this was selected.
time to reach maximum g	5.8 sec.	
maximum passenger velocity reached	180 m.p.h.	calculated using finite difference from acceleration data
steady state ω_p reached	2.16 rad/sec.	This is the column angular velocity in steady state
steady state ω_s reached	9.7 rad/sec.	This is the beam angular velocity in steady state
initial ramp up $\dot{\omega}_p$	0.2 rad/sec.^{2}	column supplied ramp up angular acceleration
initial ramp up $\dot{\omega}_s$	0.9 rad/sec.^{2}	beam supplied ramp up angular acceleration
ramp down $\dot{\omega}_p$	0.2 rad/sec.^{2}	symmetrical shape to ramp-up as seen in above plot.
ramp down $\dot{\omega}_s$	-0.9 rad/sec.^{2}	symmetrical shape to ramp-up as seen in above plot.

Table 5: ride statistics based on optimal design parameters

The cost estimate is $79,800. The material cost was the major part of this cost. This was due to the use of simple beam theory for stress analysis equations which required the use of a thick beam in order for the stress equations to be valid. The maximum stress of $\sigma_{\max} = 1.055$ MPa reached is well below the yield strength of Aluminum. Therefore, the use of finite element stress analysis or advanced plate theory would have allowed the reduction of the size of the beam while at the same time using accurate stress calculations. This would have resulted in lower cost in material. If awarded this contract, finite element would be used in order to lower the cost of material.

5.1 Future work and possible design improvement

The following are items that can be improved in the current design given additional time to perform

1. The beam and column weight can be reduced significantly by using plate shell stress analysis. This should reduce the material cost. This design used simple beam theory stress analysis which required the use of thick beam. This caused the beam to become too thick. It will be possible to have thinner beam and still not reach the yield strength. Using finite element method will allow this investigation.

2. There are additional possible cross sections to consider for failure analysis. This design concentrated on the most likely section based on beam theory. Using finite element software will allow one to more easily analyze the full structure more easily than was done in current design based on simple beam theory.

3. Torsional and twisting stress analysis were not addressed in this design due to time limitation. It is however expected that the beam will fail in bending.

6   Appendix

6.1   Use of simulator to validate different design parameters

These are selected screen shots showing different configurations tested during simulation in order to find an optimal one. These show the effect of changing the dimensions of the structure and the spin rates.
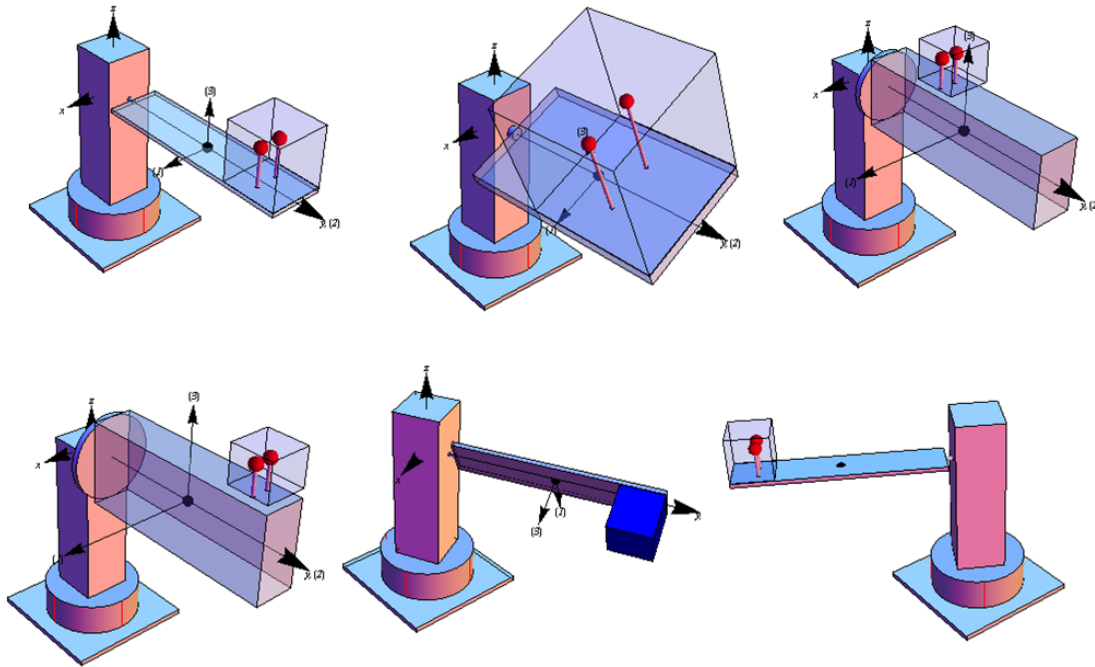

Figure 23: Changing the structure dimensions to select optimal design using simulation

6.2   References

1. Daniel C. Kammer, EMA 542 lecture notes and printed book. University of Wisconsin, Madison. 2013

2. R. C. Hibbeler. Engineering Mechanics, Dynamics. Prentice Hall, NJ 2011

3. Aluminium page at Wikipedia `http://en.wikipedia.org/wiki/Aluminium`

4. Moments of inertia page at Wikipedia `http://en.wikipedia.org/wiki/List_of_moments_of_inertia`

5. Density of materials page http://physics.info/density/

6. Beam design formulas with shear and moment diagrams book, AWC council, 2007, Washington, DC.